2000

Flow Characteristics of Oil Film in Suction Line of Refrigeration Cycle

M. Fukuta
Shizuoka University

T. Yanagisawa
Shizuoka University

K. Sawai
Matsushita Electric Industrial Co.

Y. Ogi
Shizuoka University

Fukuta, M.; Yanagisawa, T.; Sawai, K.; and Ogi, Y., "Flow Characteristics of Oil Film in Suction Line of Refrigeration Cycle" (2000). *International Refrigeration and Air Conditioning Conference.* Paper 492.
http://docs.lib.purdue.edu/iracc/492

FLOW CHARACTERISTICS OF OIL FILM IN SUCTION LINE OF REFRIGERATION CYCLE

Mitsuhiro FUKUTA*, Tadashi YANAGISAWA*,
Kiyoshi SAWAI** and Yasuhiro OGI*

* Department of Mechanical Engineering, Shizuoka University
3-5-1, Johoku, Hamamatsu, 432-8561, JAPAN
e-mail: m-fukuta@eng.shizuoka.ac.jp

** Air Conditioning Research Laboratory, Matsushita Electric Industrial Co.
3-1-1, Nojihigashi 2chome, Kusatsu, Shiga, 525-8520, JAPAN

ABSTRACT

A suction line of a refrigeration cycle with vertical upward flow is one area where the refrigeration oil tends to accumulate. This paper discusses the flow characteristics of the oil film in a pipe with the vertical upward flow. Air and oil two-phase flow is used as the first step of the study and the flow pattern of the oil film in the vertical upward flow is observed. The oil film thickness is measured with changing flow rate of both the air and oil, viscosity of the oil, diameter of the pipe and pressure in the pipe. The condition under which the oil film having a certain thickness can flow upward is proposed as a design criterion for the refrigeration cycle. A general expression with non-dimensional parameters is developed based on the criterion. In addition, measurement of the oil film thickness in a refrigeration cycle by using a capacitance sensor is introduced and the characteristic of the sensor is clarified.

INTRODUCTION

Recently, HFC refrigerants have been used in refrigeration, and high pressure refrigerants such as R410A or HFC32 tend to be used. The lubricating condition in a refrigerant compressor, therefore, becomes severe. In addition, although ester oil is often used as refrigeration oil for HFC refrigerant, hydrolysis of the ester oil sometimes causes blockage of a capillary tube. One method to improve the lubricating condition or avoid the use of the ester oil is use of immiscible oil with the refrigerant(1)(2). However, when an immiscible oil is used in the refrigeration cycle, the oil discharging with the refrigerant from a compressor tends to accumulate in a pipeline and it is difficult to return the oil to the compressor. Therefore it is necessary to consider the oil return in design of the pipeline(3). A suction line with vertical upward flow is one area where the oil tends to accumulate, because a thin oil film is entrained by gas flow in the suction line and both temperature and pressure are low in the cycle. In order to ensure the oil return, it is important to clarify the conditions under which the oil film can rise in the vertical upward flow.

In this paper, two-phase flow of the oil and air is used to examine basic characteristics of the transport of the oil film in the vertical upward flow. The flow pattern of oil film is observed and the oil film thickness is measured with changing flow rate of both the air and oil, viscosity of the oil, diameter of the pipe, and pressure in the pipe. The condition under which oil film of a certain thickness can flow upward is proposed as a design criterion. General expression with non-dimensional parameters is developed based on the criterion. In addition, measurement of oil film thickness in the refrigeration cycle and the characteristic of the sensor are discussed.

THEORETICAL ANALYSIS

The oil and gas flow in the vertical pipe is assumed to consist of an annular liquid film with thickness h surrounding a core gas flow(4). Shear stress, τ_w, on the wall of the pipe is derived as follows from the force balance in vertical direction acting on the fluid,

$$\tau_w = \{(-dP/dz) - \rho_m g\} r_0/2 \qquad (1)$$

where, r_0 is pipe inner radius and dP/dz is pressure gradient along the pipe. ρ_m is average density of the fluid and is expressed as follows by using densities ρ_g and ρ_l of gas and liquid.

$$\rho_m = \rho_g r_i^2/r_0^2 + \rho_l\{1 - (r_i^2/r_0^2)\} \qquad (2)$$

r_i in Eq.(2) is radius of an interface between the liquid film and the gas core ($r_i = r_0 - h$). Also, force balance acting on the liquid film is reduced to the following equation under assumption of laminar flow of the liquid film.

$$-\mu_l\left(\frac{dw_l}{dr}\right) = \tau_w \frac{r_0}{r} + \left\{\rho_l g - \left(-\frac{dP}{dz}\right)\right\}\frac{r_0^2 - r^2}{2r} \qquad (3)$$

where, r is radius ($r_i < r < r_0$) and μ_l is viscosity of liquid. w_l is velocity of liquid film and is expressed as follows by integration of Eq.(3) and using non-slip condition on the wall.

$$w_l = (1/\mu_l)\left[\tau_w r_0 \ln(r_0/r) - \{r_0^2 - r^2 - 2r_0^2 \ln(r_0/r)\}\{\rho_l g - (-dP/dz)\}/4\right] \qquad (4)$$

Mass flow rate of the liquid, G_l, is derived as follows,

$$G_l = 2\pi\rho_l \int_{r_i}^{r_0} r w_l dr$$

$$= \frac{\pi}{\nu_l}\left[\tau_w r_0\left\{r_i^2 \ln\left(\frac{r_i}{r_0}\right) + \frac{r_0^2 - r_i^2}{2}\right\} + \{\rho_l g - (-dP/dz)\}\left\{\frac{r_0^2 r_i^2}{2}\ln\left(\frac{r_i}{r_0}\right) + \frac{(r_0^4 - r_i^4)}{8}\right\}\right] \qquad (5)$$

where, ν_l in Eq.(5) is kinematic viscosity of the liquid. When the liquid film is thin enough ($1 >> h/r_0$), Eq.(5) is approximated as the following equation.

$$G_l = (\pi r_0/\nu_l)\left[\tau_w h^2 + \{\rho_l g - (-dP/dz)\}(h^3/3)\right] \qquad (6)$$

EXPERIMENT

Figure 1 shows a schematic diagram of the experimental setup. The oil and air are used in the first step of the study. The test pipe is acrylic of length 1.3 m, and is set vertically. The air is fed through a check valve from an air compressor to the bottom of the test pipe. The air flow rate is controlled by a needle valve and is measured by a rotameter. The oil is introduced at a mixer located near the bottom. The mixer is a double tube with eight holes on the inner pipe wall (test pipe) in two steps so that a uniform oil film is created on the internal circumference of the pipe. The oil is stored in another acrylic pipe, and is fed to the mixer by pressurized air. Flow rate of the oil is adjusted by a needle valve and is measured by the change of oil height in the storage pipe. A valve is connected at the end of the test pipe to control the pressure in the test section. The oil leaving the test pipe is separated from the air flow by an oil separator located at the exit of the test pipe and the air is released to the atmosphere. When atmospheric pressure is used, the test pipe is divided into three lengths with the middle length sandwiched by the pipes at each end so that the middle length can be removed. After the oil film flow reaches steady state, the middle length is removed quickly and the average oil film thickness on the inner surface is measured by weighing the oil remaining in the pipe. In addition, two thin electrodes (12.7x150 mm each) facing each other are pasted on the outer surface of the upper part of the pipe in order to measure capacitance between them. The capacitance will increase with the increase of the oil film thickness. The output of the sensor is calibrated to give the oil film

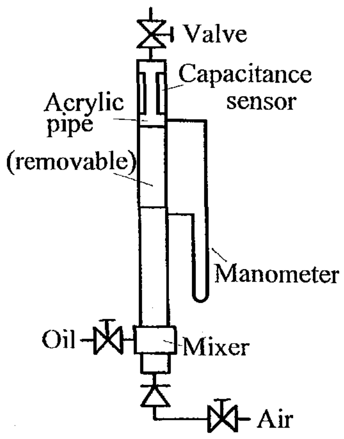

Fig.1 Test section

Table 1 Test conditions

Inner diameter of test pipe	8 mm, 10 mm
Oil (viscosity under test condition)	Mineral oil VG56 (260mm²/s), VG20 (73mm²/s)
Gauge pressure in pipe	0, 101 kPa
Volumetric flux of air	8~36 m/s
Volumetric flux of oil	0~0.25 mm/s

thickness measured by the method described. Under pressurized conditions, the test section is replaced by a single pipe and only the capacitance sensor is used to measure the film thickness. The pressure in the pipe does not affect the output of the sensor in the range tested. The pressure in the pipe is measured by a Bourdon gauge and the pressure drop between both ends of the test section is measured by a manometer.

In the experiment, the flow pattern of the oil film is observed and the average film thickness and the pressure drop are measured with changing flow rate of both air and oil, viscosity of oil, diameter of pipe and pressure in pipe. Test conditions are shown in Table 1.

RESULTS AND DISCUSSION

Fundamental Characteristics

The flow pattern of the oil film annular flow in the vertical pipe is classified into the following regimes in this study.

Ⅰ [L-D regime]: Large disturbance wave exists on the surface of liquid film.
Ⅱ : Transient regime between regime Ⅰ and Ⅲ.
Ⅲ[Ri regime]:Pipe wall is covered by liquid film with small ripple.
Ⅳ[N-W regime]: Liquid film is broken and whole surface is not wetted (Non-Wetting).

The flow pattern is illustrated and photographs of the regimes Ⅰ and Ⅲ are shown in Fig.2.

Figure 3 shows a map of flow pattern under the condition that the oil is VG56, the pipe inner diameter is 10 mm and the pressure is atmospheric. Horizontal axis and vertical axis are volumetric flux, w_{g0} and w_{l0} (volumetric flow rate/pipe sectional area) of gas and liquid respectively. Roman numerals in Fig.3 correspond to each flow pattern regime. The gas volumetric flux (almost the same as the gas velocity) is dominant over the transition of the flow pattern from the regime Ⅰ to the regime Ⅲ. This is because the

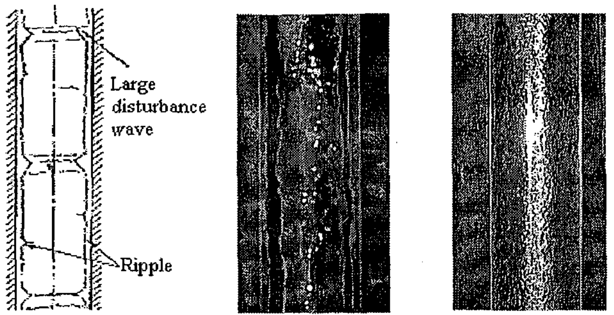

(a) Illustration (b) Regime Ⅰ (c) Regime Ⅲ

Fig.2 Flow pattern

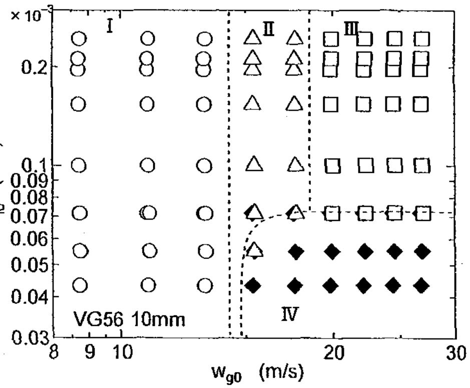

Fig.3 Flow pattern map

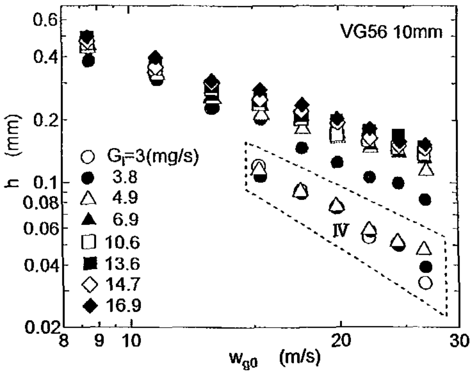

Fig.4 Oil film thickness (1)

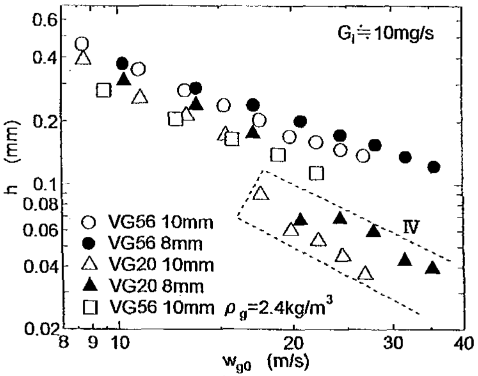

Fig.5 Oil film thickness (2)

transition of the flow pattern is governed by the oil film thickness and under the constant gas pressure the oil film thickness is influenced by the gas velocity as shown later. The flow pattern of the regime IV is observed when the oil flow rate is small and the gas velocity is large. In this regime, one or two stream lines of oil go up along the pipe wall. On the other hand, when the oil flow rate increases too much, the large disturbance wave tends to plug the section of pipe and Floss or Slug flow is observed. In the case of the smaller pipe diameter with the low viscosity oil, the gas velocity is also dominant over the transition of flow pattern. The regime IV spreads to the region where the oil flow rate is large when the pipe diameter is large and the oil viscosity is low. Note that the oil stream flow (regime IV) will change according to the surface tension of oil and affinity with the wall, and further testing is required for this type of flow.

Figure 4 shows the relationship between the volumetric flux of gas and the average oil film thickness under several oil flow rates. The pipe inner diameter is 10 mm, the oil is VG56 and the pressure is atmospheric. The oil film thickness decreases with the increase of the gas velocity. On the other hand, the oil film thickness increases with the increase of the oil flow rate, however, the fractional thickness increase is smaller than that of flow rate. This is because when the oil flow rate increases the large disturbance wave appears and the oil is carried up by the large disturbance wave. The data enclosed by the dotted line in the bottom right of Fig.4 belong to regime IV. Their oil film thicknesses are small since a uniform thickness of oil film is assumed. Figure 5 shows the oil film thickness under several conditions with the oil flow rate of approximately 10 mg/s. The larger the pipe diameter, the smaller the viscosity of oil, and the larger the gas density is, the thinner the oil film becomes under the same oil flow rate.

The comparison of measured oil film thickness with the one calculated by Eq.(6) is shown in Fig.6 as a function of the pressure gradient, *-dP/dz*. Although both results show the same tendency that the oil film thickness decreases with increase of the pressure gradient, the measured ones have smaller values. The calculated result breaks off at the minimum pressure gradient under which the oil film for specified flow rate can flow upward theoretically, and the oil flow rate decreases due to reverse flow for smaller pressure

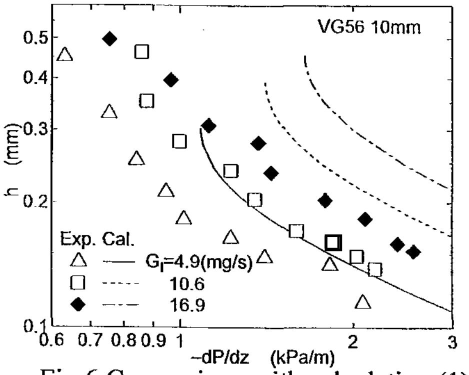

Fig.6 Comparison with calculation (1)

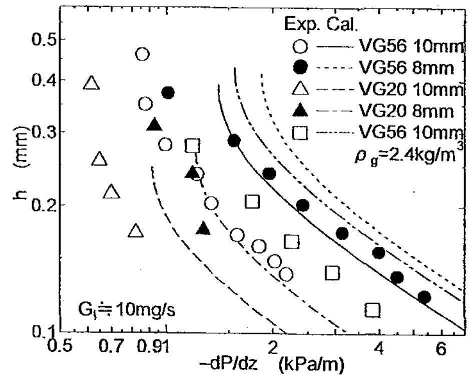

Fig.7 Comparison with calculation (2)

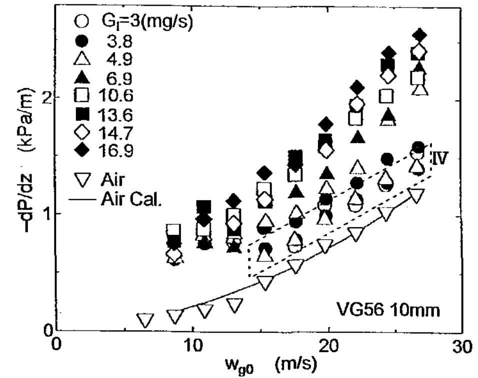

Fig.8 Pressure gradient

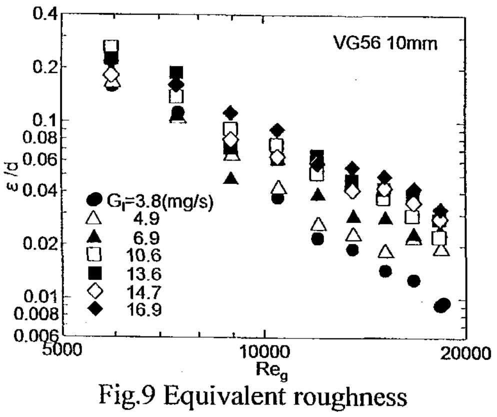

Fig.9 Equivalent roughness

gradients. On the other hand, the oil is carried up in the actual case under these smaller pressure gradients. This is because the flow of oil film is not smooth laminar flow as it is assumed in the analysis and the oil is carried up by the large wave under such conditions. Figure 7 shows the results under several conditions and these show similar trends.

Figure 8 shows the pressure gradient, $-dP/dz$, under several oil flow rates, G_l, versus the gas volumetric flux, w_{g0}. The result for a single-phase flow of air is also shown as a reference, and it has good agreement with a calculated pressure gradient using a friction coefficient estimated under turbulent conditions. The pressure gradient becomes large in comparison with that for the air-only flow when the oil flow rate increases, since the surface at the interface between oil and gas is disturbed. Therefore, it is assumed that the increase of the pressure gradient is caused by surface roughness on the pipe wall. A relative roughness ε/d, corresponding to the friction coefficient for which the calculated pressure gradient of air flow agrees with the experimental result, is estimated by the following equation.

$$\lambda = 1/\{1.74 - 2\log(2\varepsilon/d)\}^2 \qquad \mathrm{Re} > 900/(\varepsilon/d) \tag{7}$$

The equivalent relative roughness versus the Reynolds number of gas, Re_g, is shown in Fig.9. In this figure, the equivalent relative roughness increases with the decrease of the Reynolds number or gas velocity, and this agrees with actual behavior.

Criterion of Oil Transportation

As mentioned above, the oil film can flow upward in the vertical pipe if a thick oil film forms even when the gas velocity is low. However, the oil transport with such a thick oil film is not desirable in terms of pressure drop in the suction line, heat transfer in heat exchangers, or amount of oil that is discharged from the compressor. Therefore, when one discusses the oil return in the vertical pipe in the refrigeration cycle, one should discuss the thickness of the oil film flowing upward, not only whether the oil film can flow upward or not. In this study, maximum allowable oil film thickness (referred as the baseline film thickness in the following) is chosen to be 0.2 mm for the time being. The conditions under which the oil film thickness is 0.2 mm in each experiment are summarized in Fig.10. The horizontal axis is the oil flow rate, G_l, and the vertical axis is the volumetric flux of gas, w_{g0}, such that the film thickness equals the baseline (=0.2 mm). The gas velocity under this condition increases with increase of the oil flow rate. The gas velocity is larger when the pipe diameter is small, the oil viscosity is large and the gas density is small. This dependence is re-arranged into a relationship between the gas Reynolds number, Re_g, and the liquid film Reynolds number, Re_f, as shown in Fig.11. The liquid Reynolds number is represented by the following equation.

$$\mathrm{Re}_f = 4G_l/(\pi d \mu_l) \tag{8}$$

The transport characteristics of the oil film having the baseline thickness can be partially expressed with the gas Reynolds number.

In addition, Fig.12 shows the relationship between liquid Reynolds number, Re_f, and non-dimensional shear stress[(5)], τ_i^*, on the interface, defined by

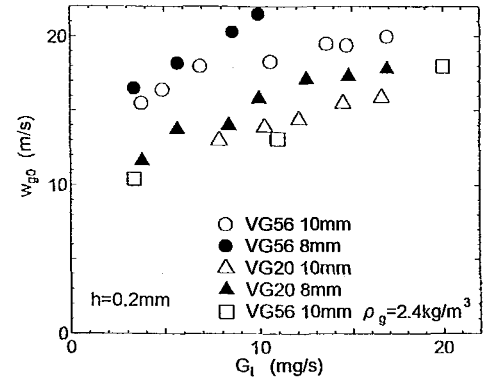

Fig.10 Gas velocity with 0.2mm oil film

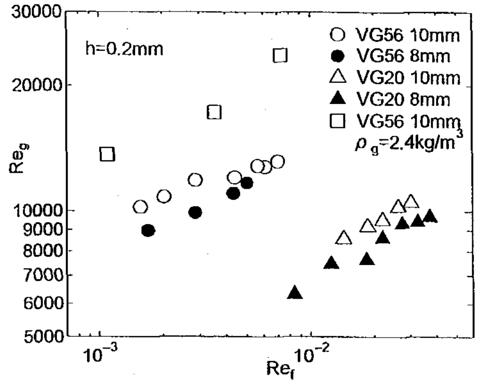

Fig.11 Relationship between Re_f and Re_g

$$\tau_i^* = \{\tau_i/(\rho_l g)\}/d' \tag{9}$$

where, τ_i is shear stress on the interface and d' is a representative length. These are expressed as follows respectively.

$$\tau_i = \{(-dP/dz) - \rho_g g\} r_i/2 \tag{10}$$

$$d' = (\nu_l^2/g)^{1/3} \tag{11}$$

In Fig.12, similar correlations are shown under different conditions, and it is found that the shear stress on the interface is the predominant factor on the transport of the oil film in the vertical pipe.

The oil flow rate transported with the baseline film thickness is assumed to be a function of the inner diameter of pipe, the gas and liquid densities, the gas velocity, and the gas and liquid viscosities. The following relationship is assumed based on dimensional analysis.

$$\mathrm{Re}_f = 10^a \mathrm{Re}_g^b (d/d')^c (\rho_g/\rho_l)^d (\mu_g/\mu_l)^e \tag{12}$$

The coefficients in Eq.(12) are derived by a regression analysis as $a = -7.2025$, $b = 3.6494$, $c = -2.2656$, $d = -1.8098$, and $e = 3.2745$. Figure 13 shows the relationship between the liquid film Reynolds number and the right hand side of Eq.(12) calculated by using these coefficients. Figure 13 shows that Eq.(12) expresses the correlation of experimental results well. By using such a correlation, the Reynolds number of gas which is required to transport the oil film with the baseline film thickness can be obtained. In order to derive a design criterion for the suction line of the upward flow in the refrigeration cycle, it is necessary to extend the correlation of Eq.(12) with the data over a wider range including oil-refrigerant two phase flow.

Measurement of Oil Film Thickness in Refrigeration Cycle

In order to get a valid correlation of Eq.(12) for the suction line in the refrigeration cycle, the measurement of oil film thickness in the refrigeration cycle is necessary. However, the calibration between the output of the capacitance sensor and the oil film thickness obtained for the air-oil two-phase flow is not satisfactory for the oil-refrigerant two-phase flow as it is, because mixing of the refrigerant into the oil changes the capacitance of oil significantly(6). Therefore, the measurement method of the oil film thickness in the refrigeration cycle by the capacitance sensor and the characteristics of the sensor are examined in this section. Figure 14 shows the experimental refrigeration cycle for the observation of the flow pattern and the measurement of oil film thickness in the suction line of the refrigeration cycle. A glass pipe is installed vertically in the suction line. The length of the pipe is 1.5 m and the inner diameter is 8.2 mm. The compressor is a rotary type and its shell has an additional volume for oil separation from the refrigerant flow. The oil stored in the shell is fed into the refrigeration cycle at the point between the condenser exit and the expansion valve. Both flow rates of the oil and the refrigerant are measured by volumetric type flowmeters. The electrodes of the capacitance sensor are pasted on the middle of the pipe. Each of them is 150x12.7 mm. The test conditions are: refrigerant is HCFC22, the oil is mineral oil (VG32), refrigerant velocity at the test section is 8.9 m/s and refrigerant density at the test section is 10.7 kg/m^3 (310kPa-abs., 30℃) or 14.6 kg/m^3

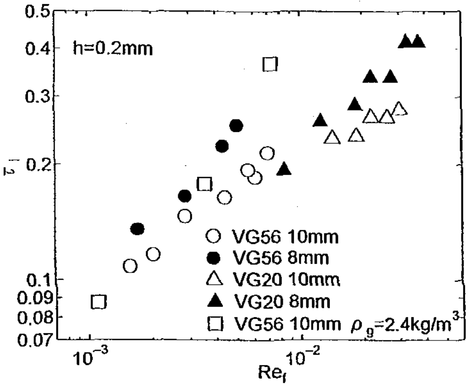

Fig.12 Relationship between Re_f and τ_i^*

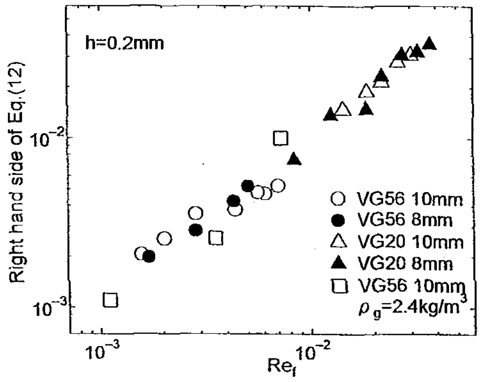

Fig.13 Correlation in Eq.(12)

(570kPa-abs., 30℃).

When the oil starts to mix into the refrigeration cycle from a condition of no oil mixing and the oil film comes up to the position of the capacitance sensor, the output of the capacitance sensor starts to increase. This time history of the sensor output is shown in Fig.15. The time of the period where the output increases, Δt, is the time for the front edge of the oil film to travel from the bottom to the top of the capacitance sensor. The velocity of the front edge of the oil film is calculated by dividing the sensor length by the traveling time. If this velocity is assumed to equal the average velocity of the oil film, the average oil film thickness can be calculated from the relationship between the volumetric flow rate of oil, Q_l, and the mean velocity, $\overline{w}_l$. The average oil film thickness, h, is expressed as follows.

$$h=\left\{d-\sqrt{d^2-4Q_l/(\pi\overline{w}_l)}\right\}/2 \qquad (13)$$

where, d is the inner diameter of the pipe. As shown in Fig.15, the sensor output becomes stable after the front of the oil film has passed through the sensor. Therefore, the front of the oil film is expected to have almost the same oil film thickness as that of steady state, although the flow of the front of oil is a transient condition.

Figure 16 shows the velocity of oil film versus the oil mass flow rate. The velocity increases with the increase of the flow rate and it increases steeply when the flow rate exceeds approximately 60 mg/s. As a result, the average oil film thickness calculated by Eq.(13) has decreasing slope with the oil flow rate as shown in Fig.17. However, the decrease of the oil film thickness with the increase of the oil flow rate is strange. The reason we obtained such a result is the change of flow pattern. When the oil flow rate exceeds 60 mg/s, the oil film becomes thick, the interface between the oil and the refrigerant is disturbed and becomes very rough, and a part of the oil flows faster than the bulk of the oil flow.

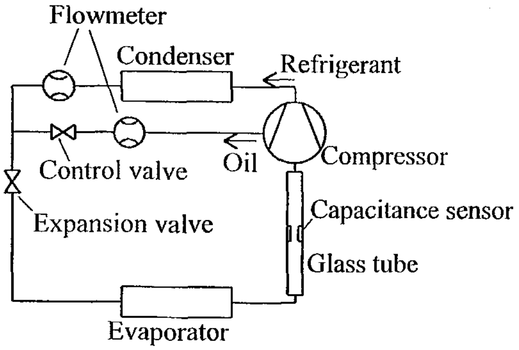

Fig.14 Experimental refrigeration cycle

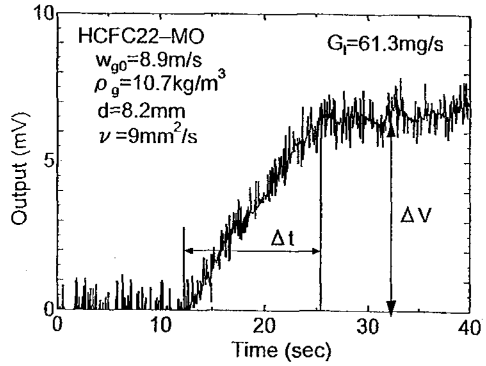

Fig.15 Change of sensor output

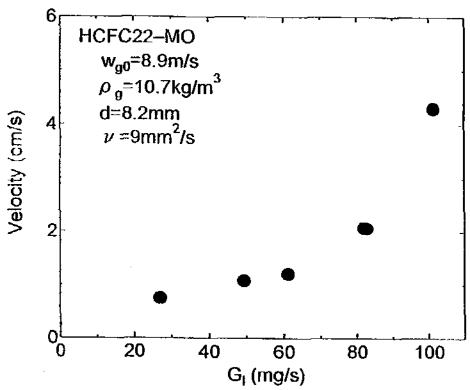

Fig.16 Average velocity of oil film

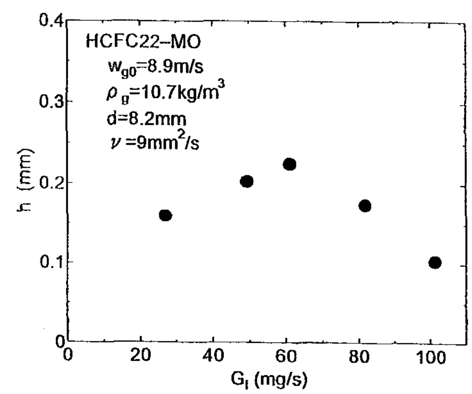

Fig.17 Oil film thickness calculated from velocity

On the other hand, the output of the sensor versus the oil flow rate is shown in Fig.18. While the output increases with the oil flow rate, the gradient of the curve becomes flat when the flow rate exceeds 60 mg/s. This is because the oil is carried by the disturbance wave in this region and the oil film thickness does not increase at the same ratio as the oil flow rate increases. Figure 19 shows the relationship between the oil film thickness and the sensor output. It is seen that there is a linear relationship between the oil film thickness and the sensor output in the region where the oil film is not so turbulent. In Fig.19, another set of the data under higher gas density, i.e. higher pressure, is also plotted. The oil film thickness under higher pressure is smaller than the other but the data shows the same trend. Once we obtain the relationship between the sensor output and the oil film thickness, we can calibrate the capacitance sensor. This calibration should be done for all combinations of oil and refrigerant which are to be measured. The measurement of the oil film thickness in the refrigeration cycle under several conditions and the development of the correlation of Eq.(12) for the suction line in the refrigeration cycle are future work.

CONCLUSIONS

As a first step of research on the oil return issue, the flow characteristics of oil film in the vertical upward flow was investigated by using air and oil. The flow pattern of oil film was observed and the average film thickness was measured under several conditions.

The flow pattern changes from a Large-Disturbance regime to a Ripple regime with the increase of the air flow velocity under constant pressure. The average film thickness decreases with the increase of the air velocity and the pressure, and also increases slightly with the increase of the oil viscosity and oil flow rate. Even in the case where the gas velocity is low, the oil can flow upward with the thick oil film. This flow pattern is not permissible in the actual refrigeration system however. Maximum oil film thickness, therefore, has to be taken into account, and the condition under which oil of a specified film thickness can flow upward is proposed as the design criterion. An empirical correlation which satisfies the criterion is obtained by using the experimental results for the air-oil two-phase flow. Although the Reynolds number of the gas phase required to carry the oil film with the specified thickness can be estimated by the correlation, further experiments for two-phase flow of the oil-refrigerant mixture is needed to apply the correlation to the suction line in the refrigeration cycle. In order to use the capacitance sensor for the measurement of the oil film thickness in the refrigeration cycle, the calibration of the sensor should be done with consideration of the characteristics of the sensor mentioned in this study.

REFERENCES

(1)S. Sekiya, et al., Proc. 1998 Int. Compr. Eng. Conf. at Purdue, (1998), p.465.
(2)M. Sunami, et al., Proc. 1996 Int. Refrig. Conf. at Purdue, (1996), p.303.
(3)S. Kawaguchi, et al., Proc. 1994 Int. Compr. Eng. Conf. at Purdue, (1994), p.535.
(4)K. Sekoguchi, Trans. of JSME, Vol.39, No.317, (1973), p.313. (in Japanese)
(5)Edited by JSME, *Gas-liquid two-phase flow technical handbook*, (1989), Corona Co., p294. (in Japanese)
(6)M. Fukuta, et al., Trans. of JSRAE, Vol.16, No.3, (1999), p.239. (in Japanese)

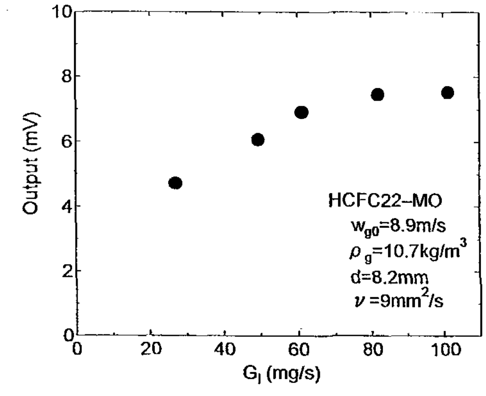

Fig.18 Output of capacitance sensor

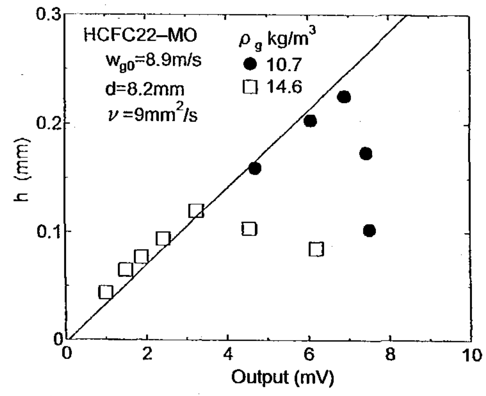

Fig.19 Calibration of capacitance sensor